

## Supplemental material

Thierry et al., <https://doi.org/10.1084/jem.20180344>

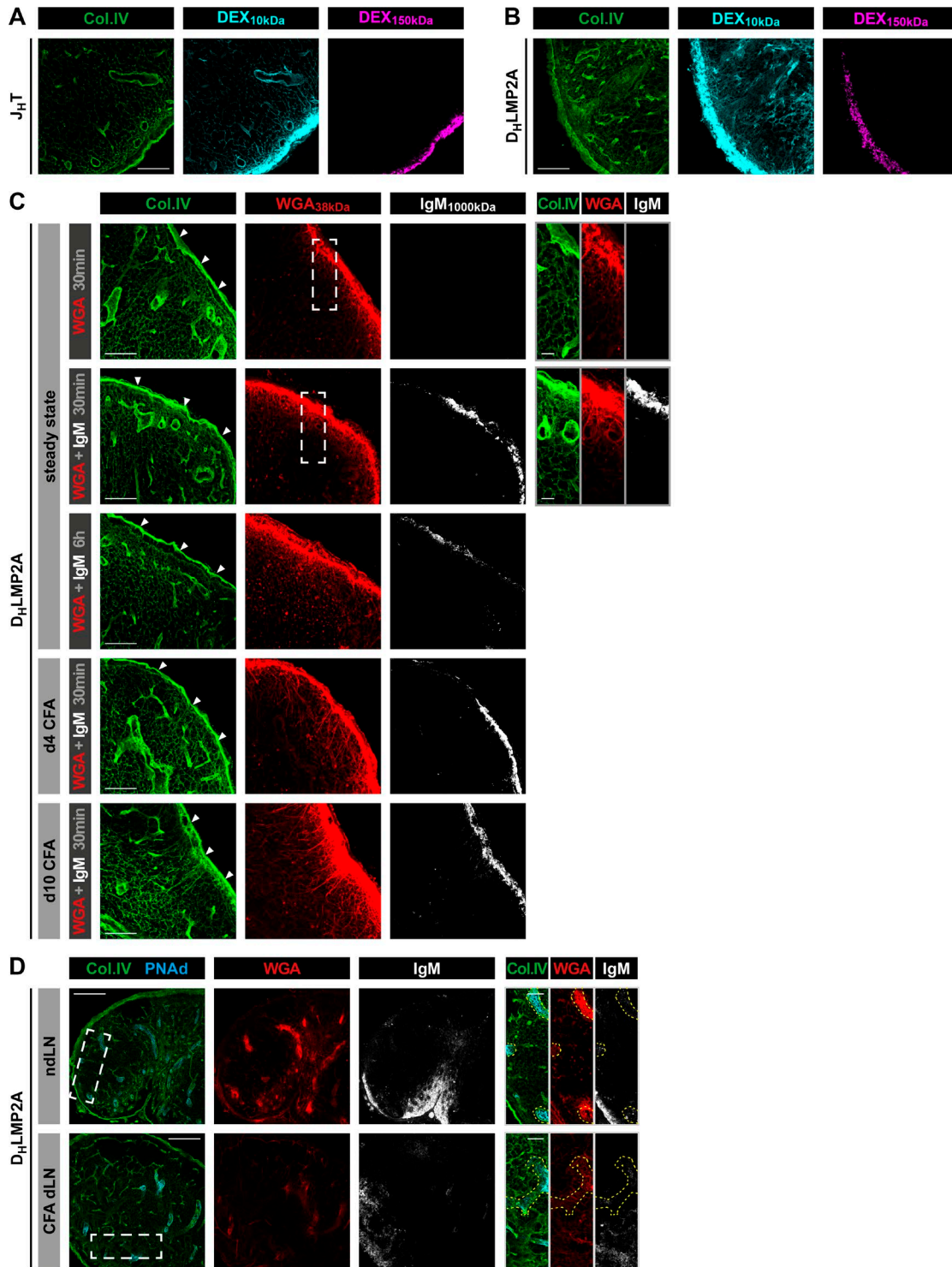


Figure S1. **Lymph- and blood-borne soluble IgM does not access the conduit system of  $D_HLMP2A$  mice.** (A and B) Two fluorescent dextrans (DEX) weighing 15 kD (blue) and 150 kD (purple) were coinjected in the ear of  $J_HL$  (A) and  $D_HLMP2A$  (B) mice. 30 min later, auricular dLNs were harvested, sectioned, and stained for collagen IV (Col.IV) expression. Bars, 100  $\mu$ m. Data represent one experiment (two mice per condition). (C) Unimmunized  $D_HLMP2A$  mice or animals that received an injection of CFA in the ear 4 or 10 d before were injected s.c. with fluorescent WGA (~38 kD)  $\pm$  IgM (~1,000 kD) in the same ear, and their auricular dLNs were harvested at the indicated time points. LN sections were stained for collagen IV and IgM. Arrowheads indicate SCS. Insets show high-magnification views of the SCS and the underlying cortex. Bars, 100  $\mu$ m (left panels); 20  $\mu$ m (right panels). Data are representative of three experiments (two mice per condition and experiment). (D)  $D_HLMP2A$  and WT mice were injected s.c. with CFA in one ear. 10 d later,  $D_HLMP2A$  mice were supplemented with the serum of the immunized WT mice over a 24-h period and injected i.v. with fluorescent WGA 5 min before the harvest of reactive and contralateral auricular LNs. Data show confocal images from LN sections stained for collagen IV, PNAd, and IgM. Insets display high-magnification views of PNAd<sup>+</sup> HEVs (yellow dashed line) and surrounding conduits. Bars, 200  $\mu$ m (left panels); 50  $\mu$ m (right panels). Data are representative of two experiments (three mice per experiment).

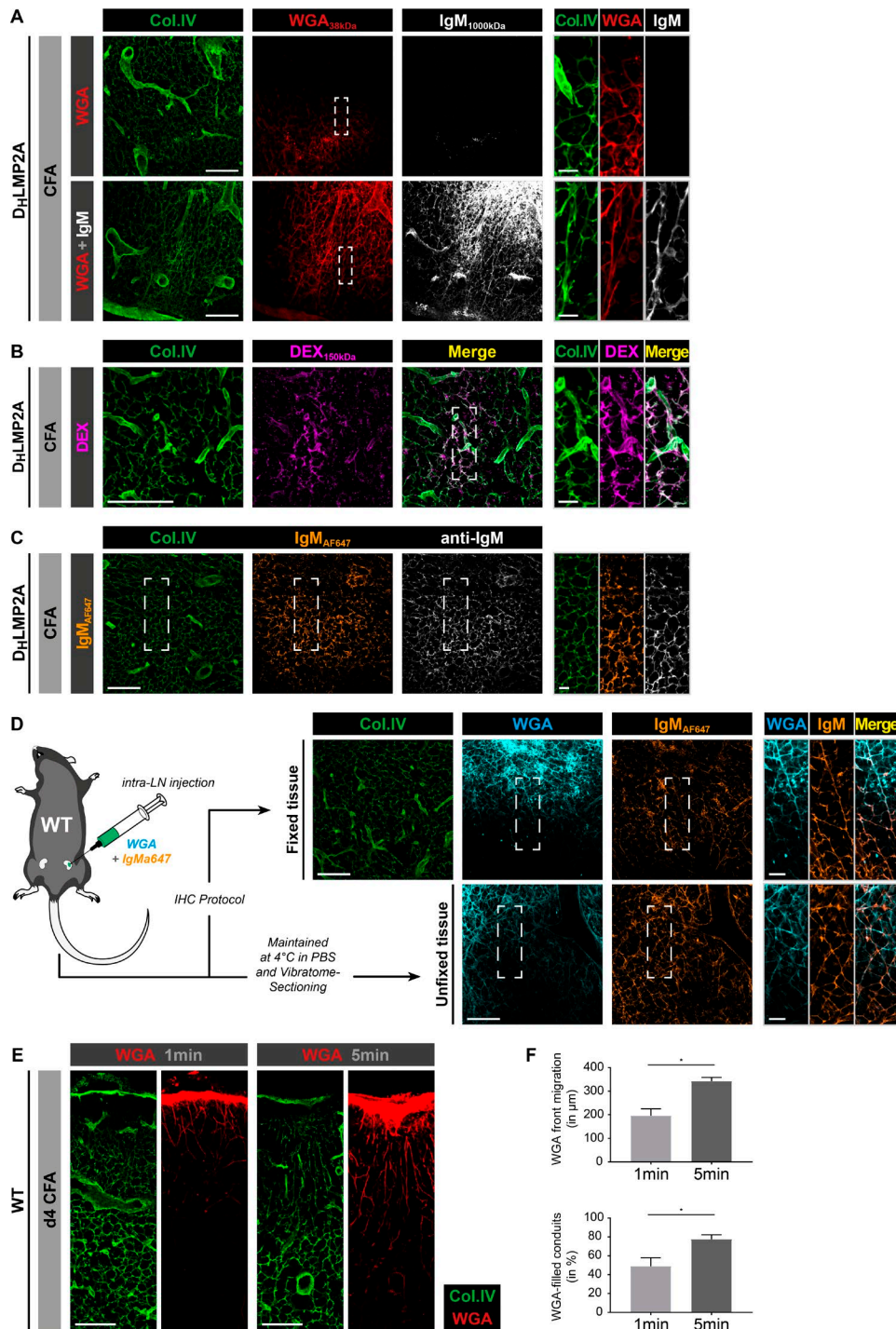


Figure S2. **The conduit system transports soluble IgM upon intranodal injection.** (A–C) D<sub>H</sub>LMP2A mice were injected s.c. with CFA at the base of the tail. 10 d later, draining inguinal LNs were surgically exposed and microinjected with fluorescent WGA with or without purified mouse IgM (A) and 150-kD fluorescent dextran (DEX; B) or fluorescent IgM (C). Data show confocal images from inguinal LN sections stained for collagen IV (Col.IV) and IgM. Insets display high-magnification views of conduits from the diffusion front. Bars, 100 μm (left panels); 15 μm (right panels). Data are representative of three experiments (two mice per condition and experiment) in A and B and two experiments (two mice per experiment) in C. (D) WT mice were immunized with CFA at the base of the tail 10 d before intranodal injection of fluorescent WGA with fluorescent IgM in reactive inguinal LNs. LNs were harvested and either fixed, sectioned, and stained for collagen IV (following the IHC protocol used in the rest of the study) or freshly maintained in cold PBS, sectioned using a vibratome, and imaged immediately. Insets display high-magnification views of conduits filled with fluorescent WGA and fluorescent IgM. Bars, 100 μm (left panels); 25 μm (right panels). Data are representative of two experiments (three mice per condition and experiment). (E) WT mice were injected with CFA in the ears 4 d before s.c. injection of fluorescent WGA in both ears. Auricular dLNs were harvested 1 and 5 min later. LN sections were stained for collagen IV expression. Bars, 100 μm. Data are representative of two experiments (six mice per experiment). (F) The average distance between the SCS and the front of WGA migration as well as the percentage of conduits filled with the fluorescent WGA (from the SCS to 400 μm below) were evaluated in the parenchyma of auricular dLNs. Results are expressed as mean ± SEM. \*, P < 0.05. Data are representative of two experiments (six mice per experiment).

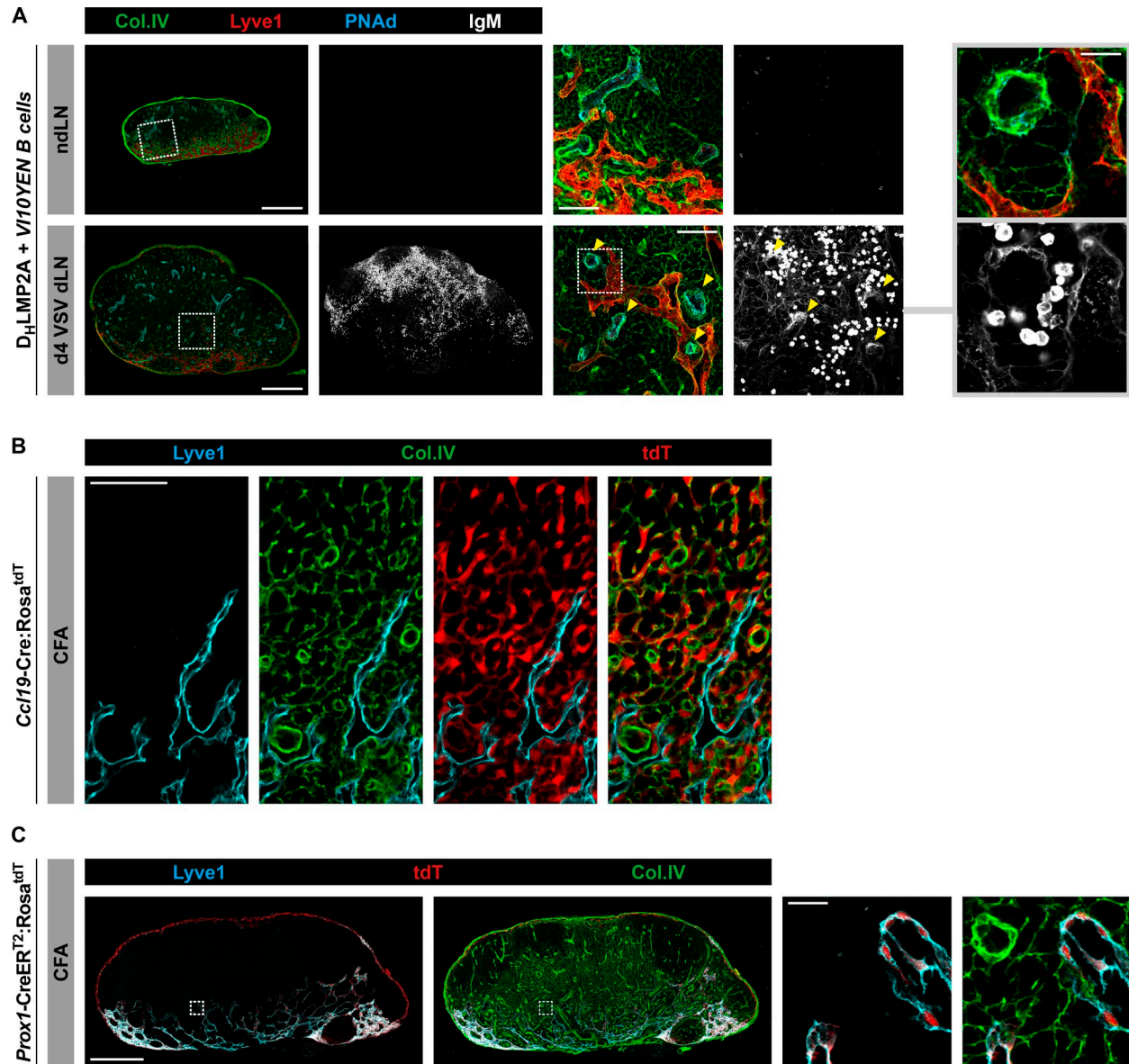


Figure S3. **The conduit system connects to the HEVs and the lymphatic sinusoids.** (A) VSV-specific VI10YEN B cells were adoptively transferred in antibody-deficient  $D_H$ LMP2A mice. Recipients were infected s.c. with VSV in the ear, and reactive and auricular ndLNs were harvested 4 d later. Sections were stained for collagen IV (Col.IV), Lyve1, PNAd, and IgM and analyzed by confocal microscopy. Insets show high-magnification views of lymphatic sinusoids and HEVs. Bars, 500  $\mu$ m (left panels); 100  $\mu$ m (middle panels); 25  $\mu$ m (right panels). Data are representative of one experiment (three mice). (B) *Ccl19-Cre:Rosa<sup>tdT</sup>* mice were injected in the ears with CFA. 10 d later, auricular LNs were stained for Lyve1 and collagen IV expression. Bars, 50  $\mu$ m. Pictures are representative of one experiment (two mice). (C) Confocal imaging of auricular reactive LN from tamoxifen-treated *Prox1-CreER<sup>T2</sup>;Rosa<sup>tdT</sup>* mice, 10 d after CFA injection in the ear. Sections were stained for Lyve1 and collagen IV expression. Insets display high-magnification views of cortical sinusoids and tdTomato-expressing lymphatic endothelial cells. Bars, 500  $\mu$ m (left panels); 25  $\mu$ m (right panels). Representative images from one experiment are shown (two mice).